mathematics

MDPI

Article

Some Important Points of the Josephson Effect via Two Superconductors in Complex Bases

Fernando S. Vidal Causanilles [1], Haci Mehmet Baskonus [2], Juan Luis García Guirao [1,3,*] and Germán Rodríguez Bermúdez [4]

[1] Departamento de Matemática Aplicada y Estadística, Universidad Politécnica de Cartagena, Hospital de Marina, 30203 Cartagena, Spain; fernandos.vidal@edu.upct.es
[2] Department of Mathematics and Science Education, Faculty of Education, Harran University, Sanliurfa 63510, Turkey; hmbaskonus@harran.edu.tr
[3] Department of Mathematics, Faculty of Science, King Abdulaziz University, P.O. Box 80203, Jeddah 21589, Saudi Arabia
[4] University Centre of Defence at the Spanish Air Force Academy, UPCT-MDE Calle Coronel Lopez Pen a, s/n, Santiago de la Ribera, 30720 Murcia, Spain; german.rodriguez@cud.upct.es
* Correspondence: juan.garcia@upct.es

Abstract: In this paper, we study the extraction of some analytical solutions to the nonlinear perturbed sine-Gordon equation with the long Josephson junction properties. The model studied was formed to observe the long Josephson junction properties separated by two superconductors. Moreover, it is also used to explain the Josephson effect arising in the highly nonlinear nature of the Josephson junctions. This provides the shunt inductances to realize a Josephson left-handed transmission line. A powerful scheme is used to extract the complex function solutions. These complex results are used to explain deeper properties of Josephson effects in the frame of impedance. Various simulations of solutions obtained in this paper are also reported.

Keywords: nonlinear perturbed sine-Gordon equation; Bernoulli sub-equation function method; complex travelling wave solutions; singular solitons

MSC: 35G16; 35G20

check for updates

Citation: Causanilles, F.S.V.; Baskonus, H.M.; García Guirao, J.L.; Bermúdez, G.R. Some Important Points of the Josephson Effect via Two Superconductors in Complex Bases. *Mathematics* **2022**, *10*, 2591. https://doi.org/10.3390/math10152591

Academic Editor: Francisco Ureña

Received: 15 June 2022
Accepted: 22 July 2022
Published: 25 July 2022

Publisher's Note: MDPI stays neutral with regard to jurisdictional claims in published maps and institutional affiliations.

Copyright: © 2022 by the authors. Licensee MDPI, Basel, Switzerland. This article is an open access article distributed under the terms and conditions of the Creative Commons Attribution (CC BY) license (https://creativecommons.org/licenses/by/4.0/).

1. Introduction

In 1962, the British physicist Brian David Josephson discovered a mathematical relation between current and voltage [1,2]. Via this relation, he explored an effect which produces a current, known as a supercurrent. This is called the Josephson effect (JE). Basically, this effect flows continuously without any voltage applied, across a device known as a Josephson junction (JJ) [3]. Moreover, this effect is also found through a tunnel based on the behavior of electrons. Then, the important properties of electrons between two superconductors were discovered. Later, Anderson and Rowell studied the Josephson tunnel's effect on the electrons [4]. They remarked that the effect should be quite sensitive to magnetic fields, and also that the effect can only occur if both metals are superconducting and should be proportional to a special point. In 1966, Zharkov investigated the Josephson tunnel effect by using a wave function arising in the Ginzburg–Landau phenomenological theory of superconductivity, which also follows from a microscopic treatment of the problem [5]. The dynamics of a long linear Josephson tunnel junction with overlap geometry was numerically investigated in [6]. The current–voltage characteristics were observed in [7]. They studied the surface losses term and the external load matching [8]. In 2006, Ha and Nakagiri proposed a damped sine-Gordon equation given as [9]:

$$u_{tt} + \alpha u_{xx} - \beta \triangle u + \gamma = \delta f.$$

Another type of this equation is given as [10–12]:

$$u_{tt} - u_{xx} + \sin(u) = \epsilon(\gamma - \alpha u_t + \beta u_{xxt}), \tag{1}$$

where $u = u(x,t), \epsilon \geq 0$. In Equation (1), $u(x,t)$ is used to define the phase difference of the electrons between the top and the bottom superconductor [13]. αu_t (ohmic losses) and βu_{xxt} terms (surface losses) are used to symbolize the energy losses. The meaning of parameters is shown in Table 1.

Table 1. Meanings of parameters.

Parameters	Meanings
γ	The applied bias current
αu_t	The ohmic losses term
βu_{xxt}	The surface losses term
ϵ	The term for definiteness

In Equation (1), if $\epsilon = 0$, it is completely converted an integrable model, and it also has a Hamiltonian structure. If $\gamma = 0$ and $\alpha = 0$,

$$u_{tt} - u_{xx} + \sin(u) = \varepsilon u_{xxt},$$

which is named the perturbed differential equation, and it is used to explain the current along a dielective barrier of the Josephson effect [9]. In 1987, Kivshar and Malomed investigated the inelastic interactions of kink properties [14,15]. They predicted the momentum and energy between the fast soliton and slow soliton. With the help of the fundamental optimal control theory, the existence of and necessary conditions for the optimal constant parameters were presented in [16]. The transposition method was used with the help of Hilbert theory and Interpolation and Variational theory [17]. Via tunnel Hamiltonian description, the Josephson current was theoretically studied in the properties of Green's function [18]. Pagano presented the fabrication technology productions of the Josephson effect in terms of weak superconductivity used to explain the properties of two superconductors [19]. Seidel introduced various types of thin film Josephson in [20]. The current–voltage characteristics are given by the standard Resistively-Shunted-Junction circuit model in [21], and produced a high-Tc superconductor Josephson junction by way of the Helium Ion Beam technique, and studied their various properties in the 10 to 40 GHz range. In this paper, our aim is to extract more complex roots of Equation (1) in a complex basis under the rules of a powerful scheme. We will determine the strain conditions from these solutions and explain a Josephson effect in impedance between two superconductors. Moreover, we try to observe how the Josephson effect may be seen via simulations.

The rest of this paper is organized as follows: the mathematical analysis of the perturbed sine-Gordon Equation (PSGE) is given in Section 1. The theoretical analysis of the scheme proposed and applied is presented in Section 2. The method is implemented to find analytical solutions of the model in Section 3. The physical properties of the solutions obtained are reported in Section 4. Some important remarks and discussions are given in Section 5. In the last section of the paper, the conclusion is presented.

2. Theoretical Analysis of Scheme

In this section, a powerful scheme, namely, the Bernoulli sub-equation function method (BSEFM) is presented to find some results. It is summarized as follows [22–24].

Step 1. We consider the following nonlinear partial differential equation (NLPDE):

$$P(u_x, u_t, u_{xt}, u_{xx}, \cdots) = 0, \tag{2}$$

where $u = u(x,t)$. If we consider the transformation formula

$$u(x,t) = U(\eta),\ \eta = kx - ct,\ k \neq 0, c \neq 0, \tag{3}$$

into Equation (2), we obtain the following nonlinear ordinary differential Equation (NODE),

$$N(U, U', U'', \cdots) = 0, \tag{4}$$

in which $U = U(\eta)$, $U' = \frac{dU}{d\eta}$, $U'' = \frac{d^2U}{d\eta^2}, \cdots$.

Step 2. According to general properties of BSEFM, the test function of solution of Equation (4) is considered as:

$$U(\eta) = \sum_{i=0}^{n} a_i F^i = a_0 + a_1 F + a_2 F^2 + \cdots + a_n F^n, \tag{5}$$

where F is defined as Bernoulli differential equation given by:

$$F' = bF + dF^M,\ b \neq 0,\ d \neq 0,\ M \neq 0,\ M \neq 1, \tag{6}$$

where $F = F(\eta)$ has the following two important solutions:

$$\begin{aligned} F(\eta) &= \left[\frac{-d}{b} + \frac{E}{e^{b(M-1)\eta}}\right]^{\frac{1}{1-M}},\ b \neq d \\ F(\eta) &= \left[\frac{(E-1) + (E+1)\tanh\left(\frac{b(1-M)\eta}{2}\right)}{1 - \tanh\left(\frac{b(1-M)\eta}{2}\right)}\right]^{\frac{1}{1-M}},\ b = d. \end{aligned} \tag{7}$$

b, d and a_i will be determined later. Putting Equation (5) into Equation (4), we obtain an algebraic equation of F given as:

$$\Omega(F) = \rho_s F^s + \cdots + \rho_1 F + \rho_0 = 0. \tag{8}$$

Step 3. When we consider that the coefficients of $\Omega(F)$ equal zero, we find a system of algebraic equations of F given as:

$$\rho_i = 0,\ i = 0, \cdots, s. \tag{9}$$

Solving this system, we find the values of $a_0, \cdots, a_n$ which produce some analytical solutions to Equation (2).

3. Applications

In this part, we investigate the complex solutions of Equation (1) by using BSEFM. Considering the wave transformation defined by:

$$u(x,t) = U(\xi),\ \xi = kx - ct, \tag{10}$$

where $k \neq 0,\ c \neq 0$ for Equation (1), we convert it to the following NODE:

$$\epsilon\beta c k^2 U''' + (c^2 - k^2)U'' - \alpha\epsilon c U' + U - \frac{1}{6}U^3 - \epsilon\gamma = 0. \tag{11}$$

According to the Balance principle, a relation between M and n is obtained as $3M = 2n + 3$. The following cases are derived from $3M = 2n + 3$.

Case-1 When $M = 3, n = 3$, it produces the first test function of solution formula as:

$$U(\xi) = a_0 + a_1 F + a_2 F^2 + a_3 F^3, \tag{12}$$

in which $F' = bF + dF^3$ and also $b \neq 0,\ d \neq 0$. Putting Equation (12) into Equation (11), we extract the following cases:

Case-1.1a Under the term of $b \neq d$, we obtain the following parameters values:

$$\gamma = 0,\ c = -\frac{i\sqrt{\frac{3}{7} - 4b^2k^2}}{2b},\ a_3 = -\frac{i\sqrt{\frac{3}{2}}d^{\frac{3}{2}}}{b^{\frac{3}{2}}},\ \alpha = \frac{187i}{15\sqrt{7}\epsilon\sqrt{3 - 28b^2k^2}},$$
$$a_0 = 0,\ a_1 = -\frac{3i\sqrt{\frac{3}{2}}\sqrt{d}}{\sqrt{b}},\ a_2 = 0,\ \beta = -\frac{i}{30\sqrt{7}b^2k^2\epsilon\sqrt{3 - 28b^2k^2}}\cdot.$$

These parameters produce the following complex function solution to the Equation (1):

$$u_1(x,t) = -\frac{i\sqrt{\frac{3}{2}}\sqrt{d}\left(3b + \frac{d}{-\frac{d}{b} + EE\exp\left(-2b\left(kx + \frac{it\sqrt{\frac{3}{7} - 4b^2k^2}}{2b}\right)\right)}\right)}{b^{3/2}\sqrt{-\frac{d}{b} + E\exp\left(-2b\left(kx + \frac{it\sqrt{\frac{3}{7} - 4b^2k^2}}{2b}\right)\right)}}\cdot. \tag{13}$$

Strain conditions of Equation (13) are $b > 0$ and $d > 0$ for a valid solution. Various simulations of Equation (13) may be observed in Figures 1–3.

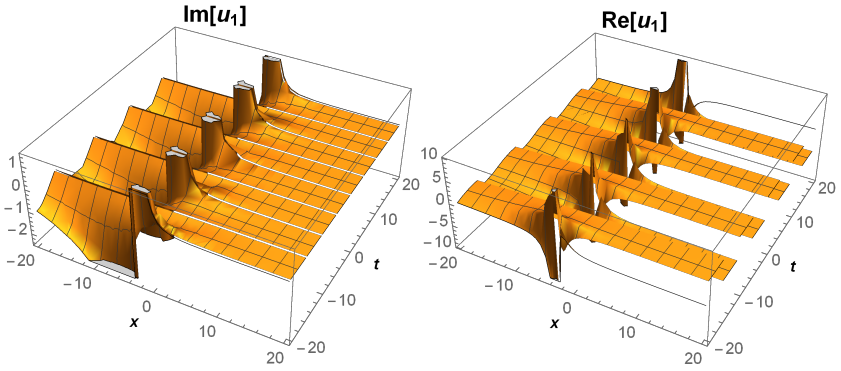

Figure 1. The 3D figures of Equation (13).

Case-1.1b Taking $b = d$ and $\gamma = 0, a_0 = 0,\ a_1 = -\frac{3i\sqrt{\frac{3}{2}}\sqrt{d}}{\sqrt{b}},\ a_2 = 0, \alpha = \frac{187i}{15\sqrt{7}\epsilon\sqrt{3-28b^2k^2}}$, $c = -\frac{i\sqrt{\frac{3}{7}-4b^2k^2}}{2b},\ a_3 = -\frac{i\sqrt{\frac{3}{2}}d^{\frac{3}{2}}}{b^{\frac{3}{2}}},\ \beta = -\frac{i}{30\sqrt{7}b^2k^2\epsilon\sqrt{3-28b^2k^2}}$, these parameters produce the hyperbolic function solution to Equation (1):

$$u_2(x,t) = -\frac{i\sqrt{\frac{3}{2}}\left(3d + \frac{d\left(1+\tanh\left(d\left(kx+\frac{it\sqrt{\frac{3}{7}-4d^2k^2}}{2d}\right)\right)\right)}{E-1-(E+1)\tanh\left(d\left(kx+\frac{it\sqrt{\frac{3}{7}-4d^2k^2}}{2d}\right)\right)}\right)}{d\sqrt{\frac{E-1-(E+1)\tanh\left(d\left(kx+\frac{it\sqrt{\frac{3}{7}-4d^2k^2}}{2d}\right)\right)}{1+\tanh\left(d\left(kx+\frac{it\sqrt{\frac{3}{7}-4d^2k^2}}{2d}\right)\right)}}}\cdot. \tag{14}$$

In Equation (14), E is a nonzero real constant. For Equation (14), several simulations may be seen in Figures 4–6.

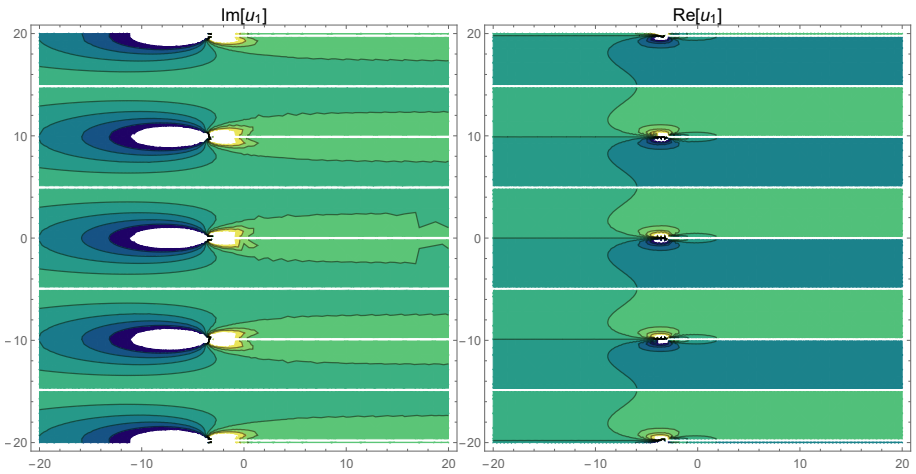

Figure 2. The contour figures of Equation (13).

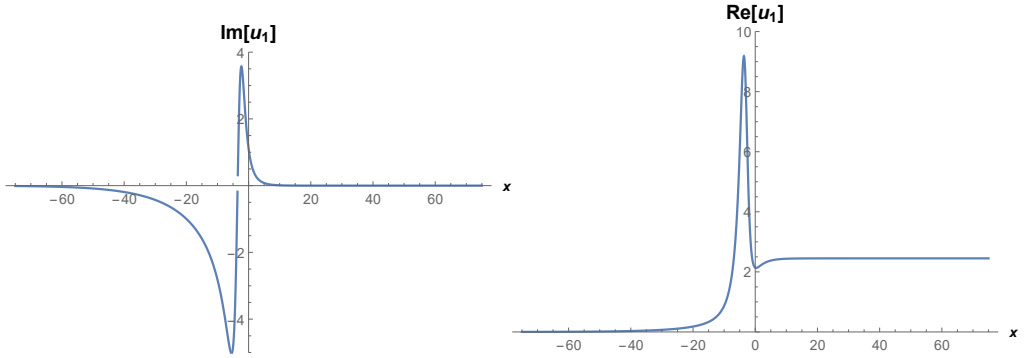

Figure 3. The 2D figures of Equation (13).

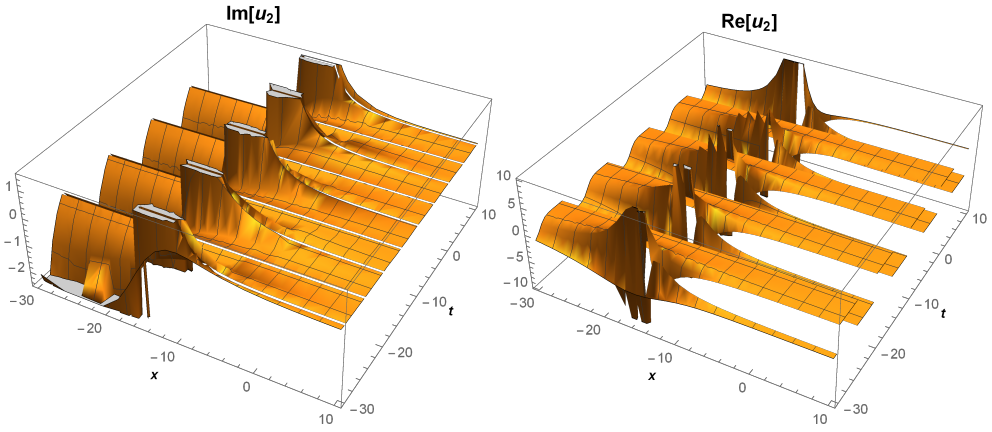

Figure 4. The 3D figures of Equation (14).

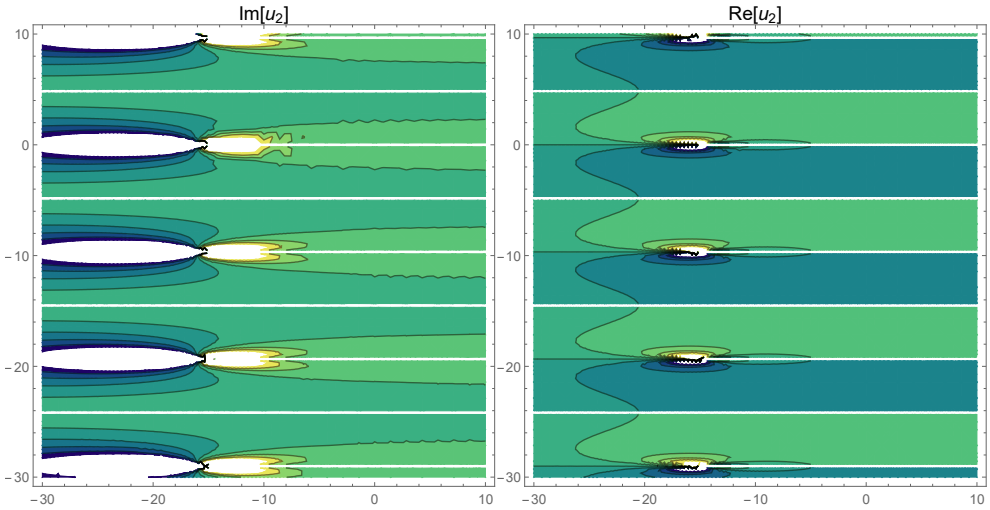

Figure 5. The contour figures of Equation (14).

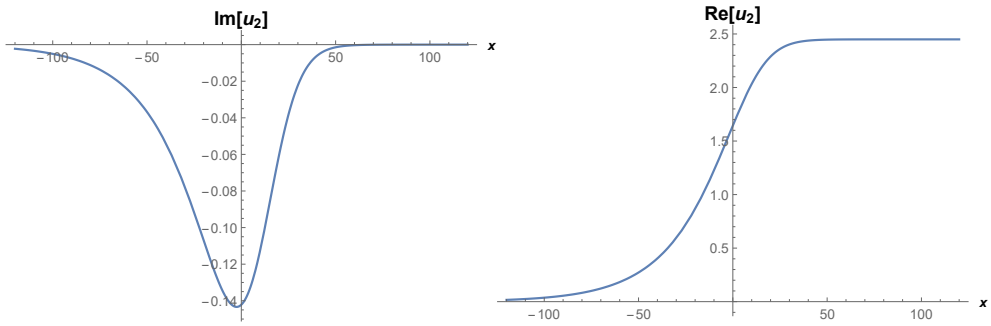

Figure 6. The 2D figures of Equation (14).

Case-1.1c If we consider other coefficients such as $a_2 = 0, \gamma = 0, a_3 = -\frac{i\sqrt{6}d^{\frac{3}{2}}}{b^{\frac{3}{2}}}, \beta = -\frac{i}{15\sqrt{7b^2k^2\epsilon}\sqrt{-7b^2k^2-1}}, a_0 = 0, a_1 = 0, c = -\frac{i\sqrt{-b^2k^2-\frac{1}{7}}}{b}, \alpha = \frac{71i}{15\sqrt{7\epsilon}\sqrt{-7b^2k^2-1}}$, we obtain the exponential function solution to Equation (1):

$$u_3(x,t) = -\frac{i\sqrt{6}d^{3/2}}{b^{3/2}}\left(-\frac{d}{b} + Ee^{-2b\left(kx+\frac{it\sqrt{-b^2k^2-\frac{1}{7}}}{b}\right)}\right)^{-\frac{3}{2}}, \tag{15}$$

in which E is a non zero reel constant and $b \neq d$. From solution (15), several simulations may be plotted by Figures 7 and 8.

Case-1.1d For $b = d$, considering $a_3 = -\frac{i\sqrt{6}d^{\frac{3}{2}}}{b^{\frac{3}{2}}}, c = -\frac{i\sqrt{-b^2k^2-\frac{1}{7}}}{b}, \alpha = \frac{71i}{15\sqrt{7\epsilon}\sqrt{-7b^2k^2-1}}$, $\gamma = 0, a_0 = 0, a_1 = 0, a_2 = 0, \beta = -\frac{i}{15\sqrt{7b^2k^2\epsilon}\sqrt{-7b^2k^2-1}}$ results in the following complex root:

$$u_4(x,t) = -i\sqrt{6}\left(\frac{-(E+1)\tanh(d\mathcal{A}) + E - 1}{1+\tanh(d\mathcal{A})}\right)^{-\frac{3}{2}}, \tag{16}$$

where $\mathcal{A} = kx + \frac{it\sqrt{-d^2k^2-\frac{1}{7}}}{d}$ and also E is a real nonzero constant.

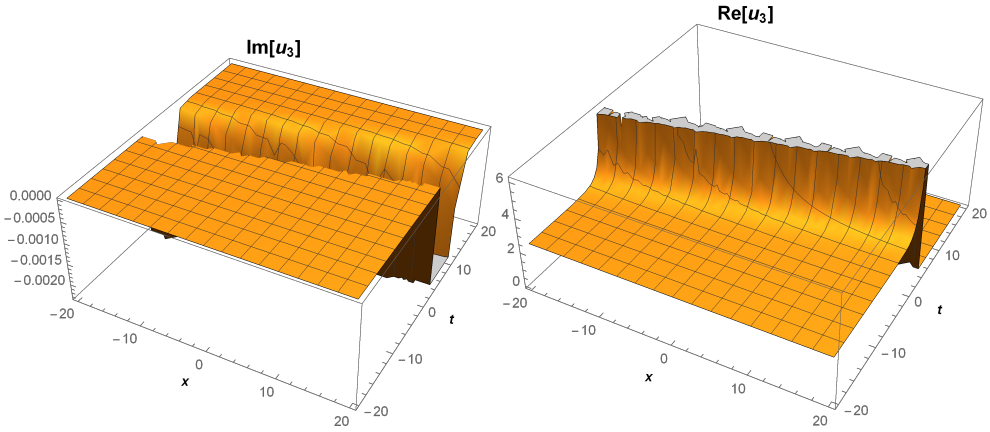

Figure 7. The 3D figures of Equation (15).

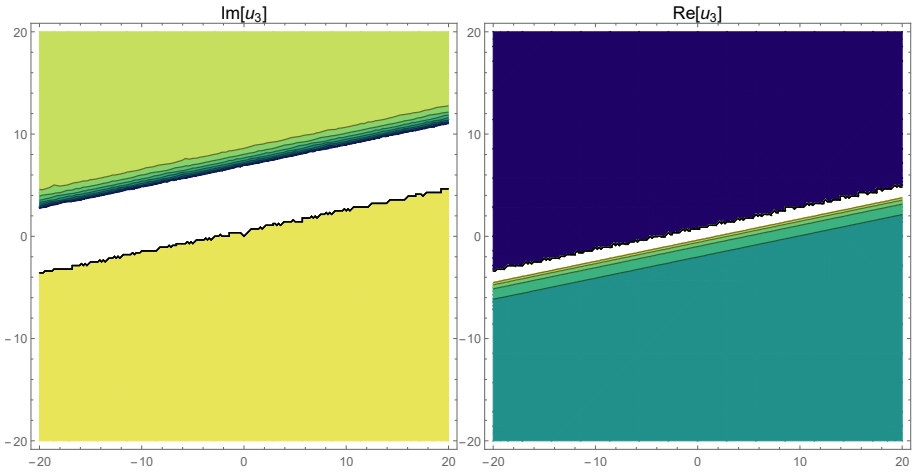

Figure 8. The contour figures of Equation (15).

Case-2 If we consider bigger values of M and n as $M = 5, n = 6$ in Equation (5), we write the second test function of the solution formula to Equation (1) as follows:

$$U(\xi) = a_0 + a_1 F + a_2 F^2 + a_3 F^3 + a_4 F^4 + a_5 F^5 + a_6 F^6, \tag{17}$$

in which $F' = bF + dF^5$ and also $b \neq 0,\ d \neq 0$. Taking Equation (17) into Equation (11), we extract the following cases of solutions:

Case-2.1a When $\beta = \frac{5i}{4\sqrt{21}b^2k^2\epsilon\sqrt{5-84b^2k^2}}, c = \frac{i\sqrt{\frac{5}{21}-4b^2k^2}}{2b}, a_0 = 0, a_1 = 0, a_2 = -\frac{4i\sqrt{6}\sqrt{d}}{\sqrt{b}}$, $a_3 = 0, \gamma = 0, a_4 = 0, a_5 = 0, \alpha = -\frac{11i}{\sqrt{21}\epsilon\sqrt{5-84b^2k^2}}, a_6 = -\frac{5i\sqrt{6}d^{\frac{3}{2}}}{b^{\frac{3}{2}}}$, we extract the following solution:

$$u_5(x,t) = -\frac{i\sqrt{6}\sqrt{d}\left(4b + \frac{5d}{-\frac{d}{b}+Ee^{-4bkx+2it\sqrt{\frac{5}{21}-4b^2k^2}}}\right)}{b^{3/2}\sqrt{-\frac{d}{b}+Ee^{-4bkx+2it\sqrt{\frac{5}{21}-4b^2k^2}}}}, \tag{18}$$

where E is a nonzero real constant. Several figures of Equation (18) may be seen in Figures 9–11 under suitable values of parameters.

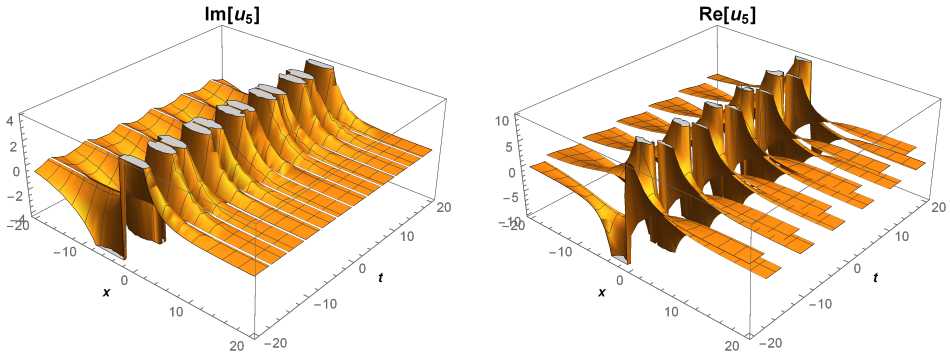

Figure 9. The 3D figures of Equation (18).

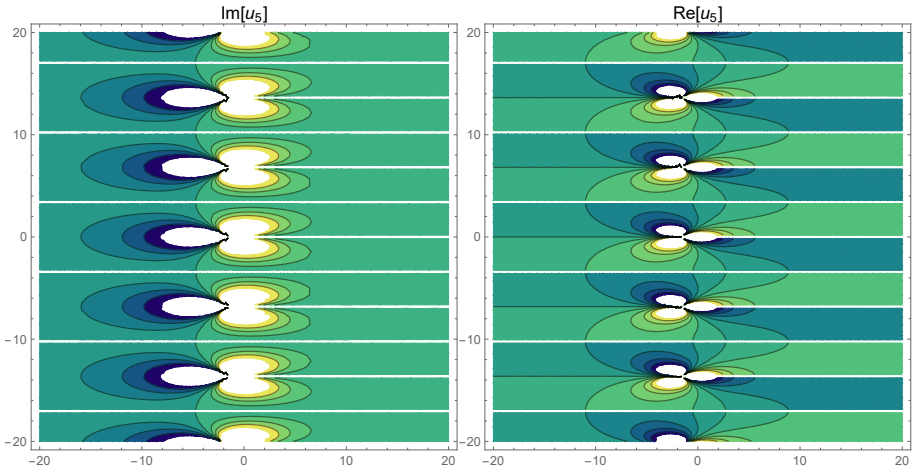

Figure 10. The contour figures of Equation (18).

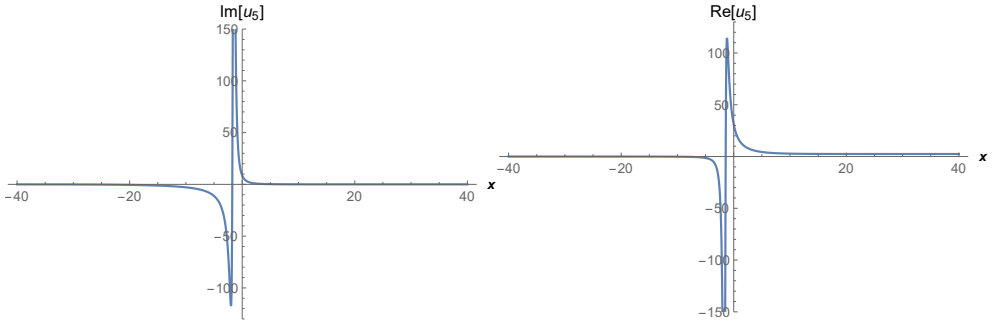

Figure 11. The 2D figures of Equation (18).

Case-2.1b When $b = d$ and $\beta = \frac{5i}{4\sqrt{21}b^2k^2\epsilon\sqrt{5-84b^2k^2}}, c = \frac{i\sqrt{\frac{5}{21}-4b^2k^2}}{2b}, b = d, a_0 = 0, a_1 = 0, a_2 = -\frac{4i\sqrt{6}\sqrt{d}}{\sqrt{b}}, a_3 = 0, a_4 = 0, \gamma = 0, \alpha = -\frac{11i}{\sqrt{21}\epsilon\sqrt{5-84b^2k^2}}, a_6 = -\frac{5i\sqrt{6}d^{\frac{3}{2}}}{b^{\frac{3}{2}}}, a_5 = 0$, gives the following exponential complex function solution:

$$u_6(x,t) = -\frac{i\sqrt{6}e^{-4dkx}\left(e^{4dkx} + 4Ee^{2it\sqrt{\frac{5}{21}-4d^2k^2}}\right)}{\left(-1 + Ee^{-4dkx+2it\sqrt{\frac{5}{21}-4d^2k^2}}\right)^{3/2}}, \tag{19}$$

in which E is a nonzero real constant.

Case-2.1c If we consider these coefficients $a_0 = 0, a_1 = 0, a_2 = \frac{3i\sqrt{\frac{3}{2}}\sqrt{d}}{\sqrt{b}}, a_3 = 0, \gamma = 0, a_4 = 0, \beta = \frac{i}{120b^2k^2\epsilon\sqrt{21-784b^2k^2}}, c = \frac{i\sqrt{\frac{3}{7}-16b^2k^2}}{4b}, a_6 = \frac{i\sqrt{\frac{3}{2}}d^{\frac{3}{2}}}{b^{\frac{3}{2}}}, \alpha = -\frac{187i}{15\epsilon\sqrt{21-784b^2k^2}}, a_5 = 0,$ we find another version of the complex function solution:

$$u_7(x,t) = \frac{i\sqrt{\frac{3}{2}}\sqrt{d}\left(3b + \frac{d}{-\frac{d}{b}+Ee^{-4bkx+it\sqrt{\frac{3}{7}-16b^2k^2}}}\right)}{b^{3/2}\sqrt{-\frac{d}{b}+Ee^{-4bkx+it\sqrt{\frac{3}{7}-16b^2k^2}}}}., \tag{20}$$

where E is a nonzero real constant. Various simulations of Equation (20) may be seen in Figures 12–14.

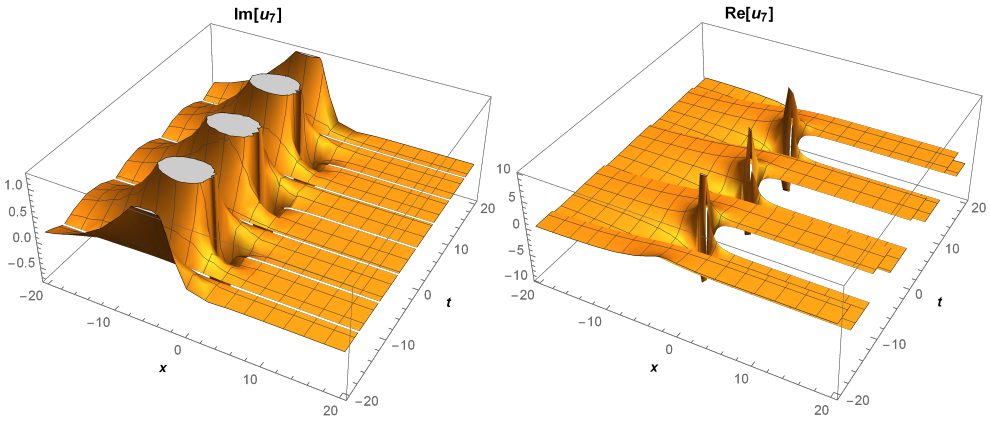

Figure 12. The 3D figures of Equation (20).

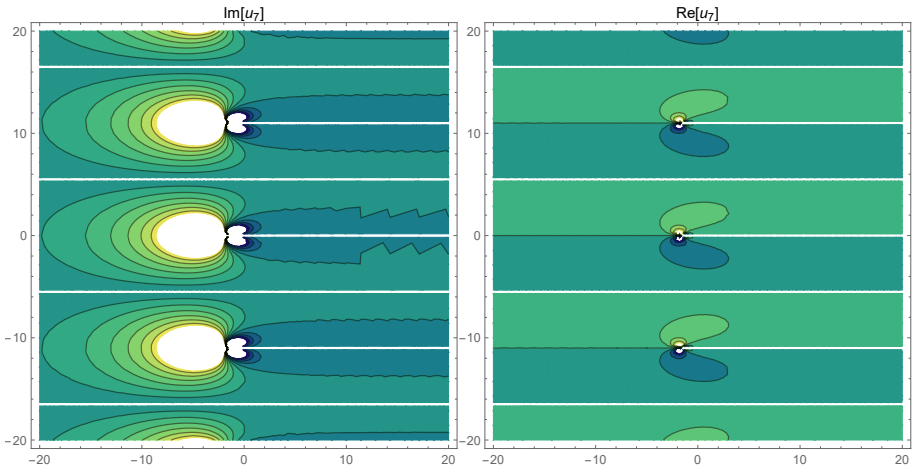

Figure 13. The contour figures of Equation (20).

Case-2.1d For $b = d$, if $a_0 = 0, a_1 = 0, a_2 = \frac{3i\sqrt{\frac{3}{2}}\sqrt{d}}{\sqrt{b}}, a_3 = 0, \gamma = 0, a_4 = 0, \beta = \frac{i}{120b^2k^2\epsilon\sqrt{21-784b^2k^2}}, c = \frac{i\sqrt{\frac{3}{7}-16b^2k^2}}{4b}, a_5 = 0, a_6 = \frac{i\sqrt{\frac{3}{2}}d^{\frac{3}{2}}}{b^{\frac{3}{2}}}, \alpha = -\frac{187i}{15\epsilon\sqrt{21-784b^2k^2}}$ gives the following complex solution:

$$u_8(x,t) = \frac{i\sqrt{\frac{3}{2}}\left(3 + \frac{1}{-1+Ee^{-4dkx+it\sqrt{\frac{3}{7}-16d^2k^2}}}\right)}{\sqrt{-1+Ee^{-4dkx+it\sqrt{\frac{3}{7}-16d^2k^2}}}}.. \tag{21}$$

Via Figures 15 and 16, various simulations of Equation (21) may be seen.

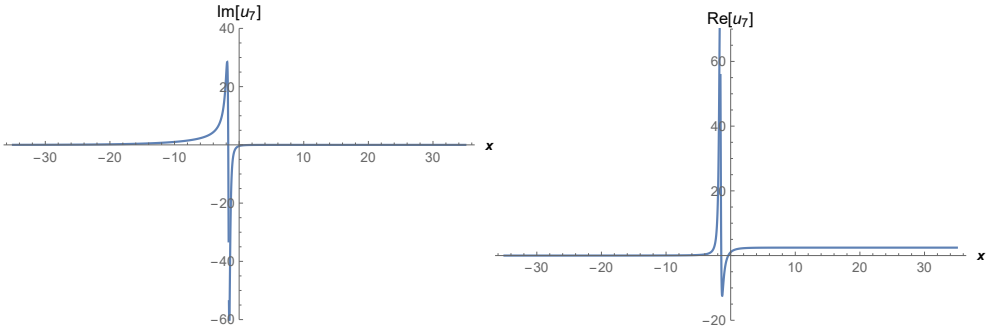

Figure 14. The 2D figures of Equation (20).

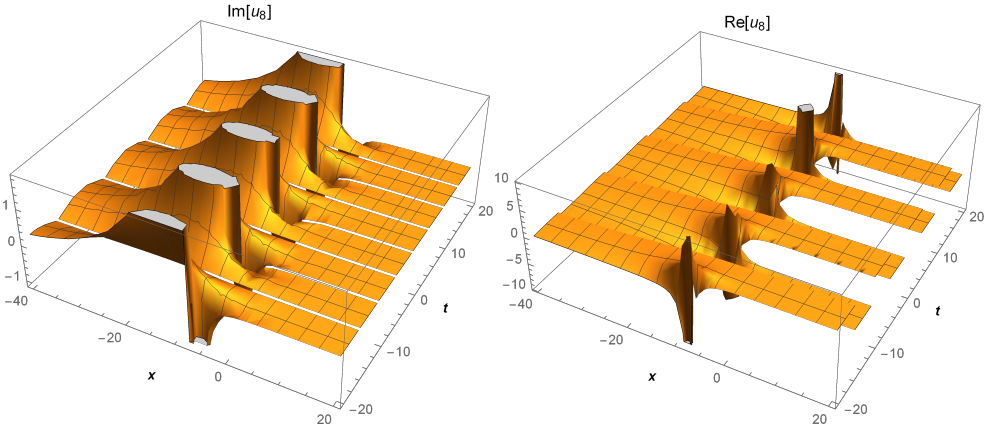

Figure 15. The 3D figures of Equation (21).

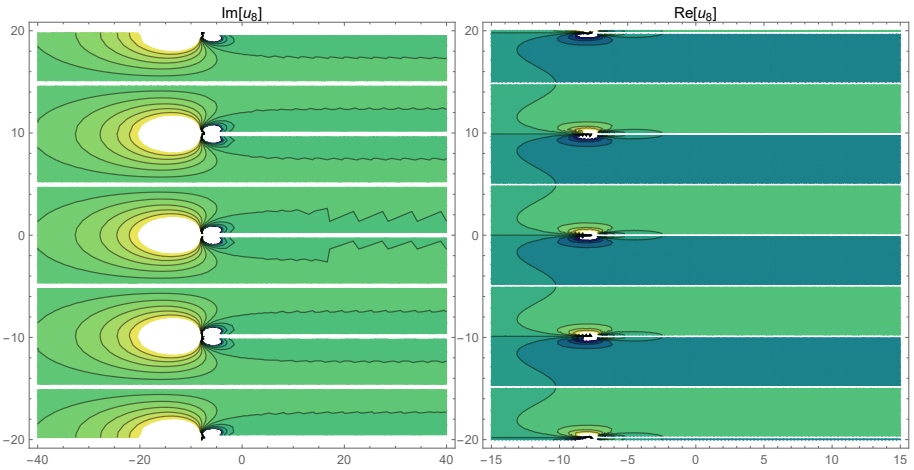

Figure 16. The contour figures of Equation (21).

Case-2.1e For these coefficients, $a_0 = 0, a_1 = 0, a_2 = 0, c = \frac{i\sqrt{-4b^2k^2-\frac{1}{7}}}{2b}, \gamma = 0, \beta = \frac{i}{60\sqrt{7}b^2k^2\epsilon\sqrt{-28b^2k^2-1}}, a_3 = 0, a_4 = 0, \alpha = -\frac{71i}{15\sqrt{7}\epsilon\sqrt{-28b^2k^2-1}}, a_6 = \frac{i\sqrt{6}d^{\frac{3}{2}}}{b^{\frac{3}{2}}}, a_5 = 0$, we extract the following result to the governing model:

$$u_9(x,t) = \frac{i\sqrt{6}d^{\frac{3}{2}}}{b^{\frac{3}{2}}\left(-\frac{d}{b} + Ee^{-4bkx+2it\sqrt{-4b^2k^2-\frac{1}{7}}}\right)^{\frac{3}{2}}} \cdot \cdot \tag{22}$$

It is observed that all these solutions verify the governing model given by Equation (1).

4. The Physical Properties

Recently, with the developing technological improvements in applied sciences, many real world problems are symbolized by using mathematical models. Traditional methods may not be given the necessary solutions of these newly presented models. In such a circumstance, these methods need to be developed or modified. In this work, we tried to find more complex solutions of the nonlinear perturbed sine-Gordon equation. This model is used to explain some important properties of the Josephson effect. Therefore, results may be used to explain some deep properties of the Josephson effect in a complex domain. From the physical point of view, while some solutions of Equations (13), (14) and (18)–(21) are complex and periodic, solution (15) is singular and (16) is a hyperbolic function and finally solution (22) is an exponential function. From Figures 1–15, it is observed that these new complex solutions are used to symbolize currents in the frame of the Josephson effect. Comparing the existing papers in the literature [10], it may be seen that these are new analytical solutions. Therefore, it is estimated that these results may be used to explain more information about the Josephson effect, which produces a current known as a supercurrent. Thus, these complex solutions are used to investigate another kind of property of the Josephson effect.

5. Some Remarks and Discussion

The main advantage of the method applied in this paper is to construct many parameters which produce new types of solutions to the governing model. It also has various strain conditions, such as parameter values, balance and satisfying the model. Moreover, this method is based on the Bernoulli differential equation. Therefore, the scheme needs to satisfy the necessary conditions of the Bernoulli model. From a theoretical point of view, in this paper, if we take the higher values of M and n which are in relationship of M and n coming from balance, such as $M = 7$ and $n = 9$, the test function solution formula for Equation (5) may be obtained as:

$$U(\xi) = a_0 + a_1F + a_2F^2 + a_3F^3 + a_4F^4 + a_5F^5 + a_6F^6 + a_7F^7 + a_8F^8 + a_9F^9. \quad (23)$$

In this equation, F has the analytical solutions of the Bernoulli differential equation given by $F' = bF + dF^7$, where F is $F(\xi)$. Comparing previous cases in this paper, we have more parameters such as a_7, a_8, a_9. These parameters may be used to produce many new types of solutions such as trigonometric, periodic, travelling, dark, bright, mixed dark–bright and complex soliton solutions to the nonlinear mathematical models. These parameters extract deeper properties of the model considered.

6. Conclusions

In this study, the nonlinear perturbed sine-Gordon equation was studied under the norms method applied. We found many different types of solution to the governing model containing the Josephson effect. The main criterion used to measure accuracy is to satisfy the model and simulate the wave behavior of the dependant variable. In this frame, it is seen that all solutions satisfied the model. The strain conditions for valid solutions are also reported. The obtained solutions are illustrated by using figures under the suitably chosen parameters. The algorithm of scheme and figures are produced via a computational package program, namely, Mathematica. When these results obtained in this paper are compared with existing solutions in the literature, it is estimated that these are used to explain the different properties of the phase difference of the electrons. These results may be used to explain the special properties of the Josephson effect in the frame of impedance between two superconductors [25]. Especially, from Figures 1, 4 and 14, the Josephson effect may be clearly observed from the left side of x. Such simulations are based on the theoretical aspect of the method. The limitation of the proposed method is based on the calculation of parameters. If we obtain more values of M and n, we find more equations for the system of equations. This is the main advantage of the method used in this paper.

From the solutions and figures, it may be estimated that such results may help to explain the Josephson effect by using complex norms. Moreover, this scheme may also be applied to other models in [26–32] as a future direction of the study. It can be inferred from the results that the method may be highly efficient for solving real world problems arising in the fields of engineering and applied science [26–49].

Author Contributions: Conceptualization, J.L.G.G. and H.M.B.; methodology, G.R.B.; investigation, F.S.V.C. All authors have read and agreed to the published version of the manuscript.

Funding: This research received no external funding.

Institutional Review Board Statement: This paper was partially supported by King Abdulaziz University with project ID: KEP-1-130-38.

Data Availability Statement: Not applicable.

Conflicts of Interest: The authors declare no conflict of interest.

References

1. Josephson, B.D. Possible new effects in superconductive tunnelling. *Phys. Lett.* **1962**, *1*, 251–253. [CrossRef]
2. Josephson, B.D. The discovery of tunnelling supercurrents. *Rev. Mod. Phys.* **1974**, *46*, 251–254. [CrossRef]
3. Available online: https://www.britannica.com/biography/Brian-Josephson (accessed on 1 January 2020)
4. Anderson, P.W.; Rowell, J.M. Probable Observation of the Josephson Tunnel Effect. *Phys. Rev. Lett.* **1963**, *10*, 230. [CrossRef]
5. Zharkov, G.F. The Josephson Tunneling Effect In Superconductors. *Soviet Physics Uspekhi* **1966**, *9*, 1–13. [CrossRef]
6. Pankratov, A.L.; Sobolev, A.S.; Koshelets, V.P.; Mygind, J. Influence of surface losses and the self-pumping effect on current-voltage characteristics of a long Josephson junction. *Phys. Rev. B* **2007**, *75*, 184516. [CrossRef]
7. Pankratov, A.L. Long Josephson junctions with spatially inhomogeneous driving. *Phys. Rev. B* **2002**, *66*, 134526. [CrossRef]
8. Pankratov, A.L. Noise self-pumping in long Josephson junctions. *Phys. Rev. B* **2008**, *78*, 024515. [CrossRef]
9. Ha, J.; Nakagiri, S.I. Identification of constant parameters in perturbed sine-Gordon equations. *J. Korean Math. Soc.* **2006**, *43*, 931–950. [CrossRef]
10. Guckenheimer, J.; Holmes, P. *Nonlinear Oscillations, Dynamical Systems and Bifurcations of Vector Fields*; Springer: New York, NY, USA, 1983.
11. Barone, A.; Paternò, G. *Physics and Applications of the Josephson Effect*; John Wiley and Sons, Inc.: New York, NY, USA, 1982.
12. Scott, A.C.; Chu, F.Y.F.; Reible, S.A. Magnetic flux propagation on a Josephson transmission line. *J. Appl. Phys.* **1976**, *47*, 3272–3286. [CrossRef]
13. Derks, G.; Doelman, A.; van Gils, S.A.; Visser, T. Travelling waves in a singularly perturbed sine-Gordon equation. *Physica D* **2003**, *180*, 40–70. [CrossRef]
14. Kivshar, Y.S.; Malomed, B.A. Many-particle effects in nearly integrable systems. *Physica D* **1987**, *24*, 125–154. [CrossRef]
15. Kivshar, Y.S.; Malomed, B.A. Dynamics of solitons in nearly integrable systems. *Rev. Mod. Phys.* **1989**, *61*, 763–915. [CrossRef]
16. Ha, J.H.; Nagiri, S. Identification problems of damped sine-gordon equations with constant parameters. *J. Korean Math. Soc.* **2002**, *39*, 509–524. [CrossRef]
17. Lions, J.L.; Magenes, E. *Non-Homogeneous Boundary Value Problems and Applications*; Springer: New York, NY, USA; Heildelberg, Germany, 1972; Volume II.
18. Sasaki, A.; Ikegaya, S.; Habe, T.; Golubov, A.A.; Asano, Y. Josephson effect in two-band superconductors. *Phys. Rev. B* **2020**, *101*, 184501. [CrossRef]
19. Pagano, S. *Introduction to Weak Superconductivity Josephson Effect: Physics and Applications*; Lecture Notes; Springer: New York, NY, USA, 2020.
20. Seidel, P. 8-High-Tc Josephson junctions. *High-Temp. Supercond.* **2011**, 317–369. [CrossRef]
21. Couëdo, F.; Amari, P.; Palma, C.F.; Ulysse, C.; rivastava, Y.K.S.; Singh, R.; Bergeal, N.; Lesueur, J. Dynamic properties of high-Tc superconducting nano-junctions made with a focused helium ion beam. *Sci. Rep.* **2020**, *10*, 10256. [CrossRef]
22. Zheng, B. Application of A Generalized Bernoulli Sub-ODE Method For Finding Traveling Solutions of Some Nonlinear Equations. *WSEAS Trans. Math.* **2012**, *7*, 618–626.
23. Baskonus, H.M.; Mahmud, A.A.; Muhamad, K.A.; Tanriverdi, T. A study on Coudrey-Dodd-Gibbon-Sawada-Kotera partial differential equation. *Math. Methods Appl. Sci.* **2022**. [CrossRef]
24. Gao, W.; Baskonus, H.M.; Mahmud, A.A.; Muhamad, K.A.; Tanriverdi, T. Studing on kudryashov-sinelshchıkov dynamical equation arising in mixtures liquid and gas bubbles. *Therm. Sci.* **2022**, *26*, 1229–1244.
25. Weisstein, E.W. *Concise Encyclopedia of Mathematics*, 2nd ed.; CRC Press: New York, NY, USA, 2002.
26. Wang, K.J. Abundant exact soliton solutions to the Fokas system. *Optik* **2022**, *249*, 168265. [CrossRef]
27. Wang, K.J. Abundant analytical solutions to the new coupled Konno-Oono equation arising in magnetic field. *Results Phys.* **2021**, *31*, 104931. [CrossRef]

28. Wang, K.J.; Wang, G. Exact traveling wave solutions for the system of the ion sound and Langmuir waves by using three effective methods. *Results Phys.* **2022**, *35*, 105390. [CrossRef]
29. Wang, K.J.; Wang, G. Variational theory and new abundant solutions to the (1+2)-dimensional chiral nonlinear Schrödinger equation in optics. *Phys. Lett. A* **2021**, *412*, 127588. [CrossRef]
30. Wang, K.J. Jing Si, Investigation into the Explicit Solutions of the Integrable (2+1)-Dimensional Maccari System via the Variational Approach. *Axioms* **2022**, *11*, 234. [CrossRef]
31. Wang, K.J.; Shi, F.; Liu, J.H.; Si, J. Application of the extended F-expansion method for solving the fractional Gardner equation with conformable fractional derivative. *Fractal* **2022**. [CrossRef]
32. Wang, K.J. Traveling wave solutions of the Gardner equation in dusty plasmas. *Results Phys.* **2022**, *33*, 105207. [CrossRef]
33. Sulaiman, T.A.; Bulut, H.; Baskonus, H.M. On the exact solutions to some system of complex nonlinear models. *Appl. Math. Nonlinear Sci.* **2020**, *6*, 29–42. [CrossRef]
34. Baskonus, H.M.; Bulut, H.; Sulaiman, T.A. New Complex Hyperbolic Structures to the Lonngren-Wave Equation by Using Sine-Gordon Expansion Method. *Appl. Math. Nonlinear Sci.* **2019**, *4*, 141–150. [CrossRef]
35. Frassu, S.; Viglialoro, G. Boundedness criteria for a class of indirect (and direct) chemotaxis-consumption models in high dimensions. *Appl. Math. Lett.* **2022**, *132*, 108108. [CrossRef]
36. Baskonus, H.M.; Kayan, M. Regarding new wave distributions of the nonlinear integro-partial ITO differential and fifth-order integrable equations. *Appl. Math. Nonlinear Sci.* **2021**, 1–20. [CrossRef]
37. Yu, X.Q.; Kong, S. Travelling wave solutions to the proximate equations for LWSW. *Appl. Math. Nonlinear Sci.* **2021**, *6*, 335–346. [CrossRef]
38. Gao, W.; Ismael, H.F.; Husien, A.M.; Bulut, H.; Baskonus, H.M. Optical Soliton solutions of the Nonlinear Schrodinger and Resonant Nonlinear Schrodinger Equation with Parabolic Law. *Appl. Sci.* **2020**, *10*, 219. [CrossRef]
39. Li, T.; Viglialoro, G. Boundedness for a nonlocal reaction chemotaxis model even in the attraction-dominated regime. *Diff. Int. Equ.* **2021**, *34*, 315–336.
40. Uddin, M.F.; Hafez, M.G.; Hammouch, Z.; Rezazadeh, H.; Baleanu, D. Traveling wave with beta derivative spatial-temporal evolution for describing the nonlinear directional couplers with metamaterials via two distinct methods. *Alex. Eng. J.* **2021**, *60*, 1055–1065. [CrossRef]
41. Uddin, M.F.; Hafez, M.G.; Hammouch, Z.; Baleanu, D. Periodic and rogue waves for Heisenberg models of ferromagnetic spin chains with fractional beta derivative evolution and obliqueness. *Waves Random Complex Media* **2020**, *31*, 2135–2149. [CrossRef]
42. Greco, A.; Viglialoro, G. Existence and Uniqueness for a Two-Dimensional Ventcel Problem Modeling the Equilibrium of a Prestressed Membrane. *Appl. Math.* **2022**. [CrossRef]
43. Bulut, H.; Akkilic, A.N.; Khalid, B.J. Soliton solutions of Hirota equation and Hirota-Maccari system by the (m+1/G')-expansion method. *Adv. Math. Model. Appl.* **2021**, *6*, 22–30.
44. Xu, L.; Aouad, M. Application of Lane-Emden differential equation numerical method in fair value analysis of financial accounting. *Appl. Math. Nonlinear Sci.* **2022**. [CrossRef]
45. Ciancio, A.; Ciancio, V.; Onofrio, A.; Flora, B.F.F. A Fractional Model of Complex Permittivity of Conductor Media with Relaxation: Theory vs. Experiments. *Fractal Fract.* **2022**, *6*, 390. [CrossRef]
46. Ciancio, A.; Ciancio, V.; Franccesso, F. Wave propagation in media obeying a thermoviscoanelastic model. *U.P.B. Sci. Bull. Ser. A* **2007**, *69*, 69–79.
47. Ciancio, A.; Yel, G.; Kumar, A.; Baskonus, H.M.; Ilhan, E. On the complex mixed dark-bright wave distributions to some conformable nonlinear integrable models. *Fractals* **2022**, *30*, 2240018. [CrossRef]
48. Ramos, H.; Rufai, M.A. An adaptive one-point second-derivative Lobatto-type hybrid method for solving efficiently differential systems. *Int. J. Comput. Math.* **2022**, *99*, 1687–1705. [CrossRef]
49. Duromola, M.K.; Momoh, A.L.; Rufai, M.A.; Animasaun, I.L. Insight into 2-step continuous block method for solving mixture model and SIR model. *Int. J. Comput. Sci. Math.* **2021**, *14*, 347–356. [CrossRef]